Kinetic Mechanism of Elongation Factor Ts-Catalyzed Nucleotide Exchange in Elongation Factor Tu†

Kirill B. Gromadski, Hans-Joachim Wieden, and Marina V. Rodnina*

Institute of Physical Biochemistry, University of Witten/Herdecke, D-58448 Witten, Germany

Received August 22, 2001; Revised Manuscript Received October 15, 2001

ABSTRACT: The interaction of *Escherichia coli* elongation factor Tu (EF-Tu) with elongation factor Ts (EF-Ts) and guanine nucleotides was studied by the stopped-flow technique, monitoring the fluorescence of tryptophan 184 in EF-Tu or of the mant group attached to the guanine nucleotide. Rate constants of all association and dissociation reactions among EF-Tu, EF-Ts, GDP, and GTP were determined. EF-Ts enhances the dissociation of GDP and GTP from EF-Tu by factors of 6×10^4 and 3×10^3, respectively. The loss of Mg^{2+} alone, without EF-Ts, accounts for a 150−300-fold acceleration of GDP dissociation from EF-Tu·GDP, suggesting that the disruption of the Mg^{2+} binding site alone does not explain the EF-Ts effect. Dissociation of EF-Ts from the ternary complexes with EF-Tu and GDP/GTP is 10^3−10^4 times faster than from the binary complex EF-Tu·EF-Ts, indicating different structures and/or interactions of the factors in the binary and ternary complexes. Rate constants of EF-Ts binding to EF-Tu in the free or nucleotide-bound form or of GDP/GTP binding to the EF-Tu·EF-Ts complex range from 0.6×10^7 to 6×10^7 M^{-1} s^{-1}. At in vivo concentrations of nucleotides and factors, the overall exchange rate, as calculated from the elemental rate constants, is 30 s^{-1}, which is compatible with the rate of protein synthesis in the cell.

Elongation factor Tu (EF-Tu)[1] promotes the binding of aminoacyl-tRNA to the ribosome during the elongation cycle of protein synthesis. EF-Tu, GTP, and aminoacyl-tRNA form a tight complex which interacts with the ribosome. Codon−anticodon interaction in the A site provides an activation signal that is transmitted to the G domain of EF-Tu and leads to GTP hydrolysis. After GTP hydrolysis and release of the aminoacyl-tRNA, EF-Tu·GDP dissociates from the ribosome. The regeneration of EF-Tu·GTP by GDP/GTP exchange requires catalysis by a nucleotide exchange factor, EF-Ts, which binds to the stable EF-Tu·GDP complex and facilitates both the dissociation of GDP and rapid binding of GTP to EF-Tu.

The structures of EF-Tu·EF-Ts complexes from *Escherichia coli* (*1*) and *Thermus thermophilus* (*2*) are known. The G domain of EF-Tu contacts the subdomain N, the N-terminal domain, and the C-terminal module of EF-Ts (helix 13), whereas domain 3 of EF-Tu is bound to subdomain C of the EF-Ts core. The structures suggest that the main elements that are crucial for the nucleotide exchange are (i) a conformational change in the P loop in the G domain of EF-Tu that leads to alterations in the binding site of the phosphate moieties of GDP/GTP, (ii) the loss of Mg^{2+} coordination, and, possibly, (iii) the change in the relative orientation of the base and/or ribose binding sites (*1*−*3*). The relative contribution of these factors to the catalysis of nucleotide exchange in EF-Tu is not known.

The kinetic mechanism of EF-Ts-catalyzed nucleotide exchange in EF-Ts has not been resolved yet, and inconsistent kinetic data were reported in the literature. Early data on the EF-Ts-dependent nucleotide exchange in EF-Tu were obtained by equilibrium isotope exchange using a rapid filtration technique (*4*, *5*). Equilibrium constants of GDP binding to EF-Tu·EF-Ts and of EF-Ts binding to EF-Tu·GDP were reported to be 6×10^4 M^{-1} and 2×10^5 M^{-1}, respectively (here and in the following, 20 °C, if not stated otherwise). The values of both bimolecular association rate constants were reported to be about 10^8 M^{-1} s^{-1}, close to the diffusion-controlled limit, whereas that of GDP dissociation from the ternary complex EF-Tu·GDP·EF-Ts was determined to 1270 s^{-1}, suggesting a 10^6-fold acceleration of GDP dissociation from EF-Tu by EF-Ts.

Different values were obtained by conventional filtration (*6*) or by stopped-flow and pressure-jump techniques using a chromophoric GDP analogue, 2-amino-6-mercaptopurine riboside 5′-diphosphate (*7*, *8*). The rate constant of GDP dissociation from the EF-Tu·GDP complex in the presence of EF-Ts measured by nitrocellulose filtration was about 120 s^{-1}, 10 times lower than that obtained using the rapid filtration approach (*6*). The analysis of the stopped-flow data yielded values for the rate constants of GDP binding to EF-Tu·EF-Ts and dissociation from the ternary complex that were about 200-fold and 3-fold lower that those reported previously (*4*), and the differences were attributed to the use of a GDP derivative (*7*). Data obtained by pressure jump using the same GDP derivative were incompatible with the earlier results (*4*, *9*) and suggested a three-step reaction where

† This work was supported by the Deutsche Forschungsgemeinschaft and the Alfried Krupp von Bohlen und Halbach Stiftung.

* To whom correspondence should be addressed: tel, +49 2302 669205; fax, +49 2302 669117; e-mail, rodnina@uni-wh.de.

[1] Abbreviations: EF, elongation factor; mant-GDP/GTP, 3′(2′)-*O*-(*N*-methylanthraniloyl)guanosine diphosphate/triphosphate; FRET, fluorescence resonance energy transfer.

10.1021/bi015712w CCC: $22.00
Published on Web 11/20/2001

the ternary complex undergoes an isomerization step that precedes GDP dissociation. The values of the bimolecular association constants were estimated to about 10^7 M^{-1} s^{-1}, and the rate constant of GDP dissociation was estimated to 375 s^{-1} (*7*). Finally, steady-state experiments using a nucleotide exchange assay in which [^{3}H]GDP liberated from EF-Tu was rapidly converted to [^{3}H]GTP by pyruvate kinase, and the rate of dissociation was measured by the GDP/GTP ratio, gave a value of 30 s^{-1} for the turnover rate constant of GDP dissociation from EF-Tu in the presence of EF-Ts (37 °C) (*10*, *11*), more than 40 times lower than that found by rapid filtration (*4*). The rate constants of GTP interaction with EF-Tu and EF-Ts were obtained by rapid filtration only (*5*) and were not verified by other methods. It was shown that filtration as a nonequilibrium technique tends to produce artifacts when rapid reactions and/or weak complexes are investigated, in particular when sequential reaction schemes are to be considered (*12*, *13*). Thus, to obtain a consistent data set for EF-Ts-catalyzed nucleotide exchange on EF-Tu, it appeared important to perform a complete kinetic analysis of the interactions among EF-Tu, EF-Ts, and guanine nucleotides using an independent, reliable approach.

In the present paper we determined the rate constants of interaction of EF-Tu with EF-Ts and GDP or GTP by the stopped-flow technique. Nucleotide binding/dissociation was studied using fluorescent derivatives of GDP/GTP, mant-GDP, or mant-GTP. Fluorescence changes of the reporter mant group were monitored either upon direct excitation of the fluorophor or upon indirect excitation via energy transfer from the single tryptophan (Trp184) in *E. coli* EF-Tu to mant. It was shown previously that nucleotide binding (*14*) and nucleotide exchange reactions in GTP binding proteins other than EF-Tu are not perturbed by the mant group (*15*). The binding of EF-Tu to EF-Ts was monitored by the fluorescence of Trp184 which has an increased mobility and solvent accessibility in the EF-Tu·EF-Ts complex compared to EF-Tu·GDP (*16*). The combination of these observables allowed us to study the partial reactions between EF-Tu, EF-Ts, and GDP/GTP individually and to determine their kinetic parameters. The results of the kinetic analysis provide a consistent mechanism of nucleotide exchange in EF-Tu and reveal the contribution of the loss of Mg^{2+} coordination to the dissociation of the nucleotide.

MATERIALS AND METHODS

Buffer and Reagents. Buffer A: 25 mM Tris-HCl, pH 7.5, 50 mM NH_4Cl, and 10 mM $MgCl_2$. All experiments were performed at 20 °C, if not stated otherwise. Chemicals were from Roche Biochemicals or Merck. Mant-GDP and mant-GTP were purchased from Molecular Probes or JenaBioScience.

EF-Tu Purification. EF-Tu was purified from *E. coli* MRE 600 by a published procedure (*17*) with some modifications. Cells were opened by sonication in buffer B (25 mM Tris-HCl, pH 7.5, 50 mM NH_4Cl, 10 mM $MgCl_2$, 0.1% PMSF, 6 mM 2-mercaptoethanol). EF-Tu was purified by ion-exchange chromatography on DEAE-Sepharose CL6B. The protein was eluted using a linear gradient of KCl (0−0.4 M) in buffer C (25 mM Tris-HCl, pH 7.5, 30 mM $MgCl_2$, 30 μM GDP, 6 mM 2-mercaptoethanol). EF-Tu-containing fractions were identified by 12% SDS−PAGE and by binding of EF-Tu·[^{3}H]GDP complexes to the nitrocellulose filters (*18*), concentrated in Centriprep YM-30 (Amicon Bioseparations), and purified further by gel filtration on Superdex 75 (HiLoad 26/60, Pharmacia) in buffer A. Fractions containing EF-Tu were concentrated, shock-frozen in liquid nitrogen, and stored at −80 °C.

Preparation of Nucleotide-Free EF-Tu. To promote the dissociation of GDP, which is tightly bound to EF-Tu and coelutes with the factor during the purification, EF-Tu·GDP was incubated in buffer D (25 mM Tris-HCl, pH 7.5, 50 mM NH_4Cl, 10 mM EDTA) for 30 min at 37 °C, and GDP was separated from EF-Tu by gel filtration on Superdex 75. Nucleotide-free EF-Tu obtained by this procedure was stable and had the same properties as untreated EF-Tu with respect to interactions with EF-Ts and guanine nucleotides (not shown). The GDP content of EF-Tu preparations was verified by RP-HPLC on C_{18}·MNP (Macherey-Nagel) in buffer E (65 mM potassium phosphate, pH 6.2, 2 mM tetrabutylammonium hydrogen sulfate, 15% acetonitrile) (*19*).

Preparation of EF-Tu·Mant-GDP, EF-Tu·Mant-GTP, and EF-Tu·EF-Ts. EF-Tu·GDP was incubated with a 10-fold excess of mant-GDP or mant-GTP in buffer A for 30 min at 37 °C with subsequent purification from the unbound nucleotide by gel filtration on a NAP-10 column (Pharmacia) (*20*). To remove GDP from EF-Tu complexes with mant-GTP, the reactions were carried out in the presence of 3 mM phosphoenolpyruvate and 0.1 mg/mL pyruvate kinase. The EF-Tu·EF-Ts complex was prepared by mixing EF-Tu and EF-Ts in equimolar amounts and was purified on Superdex 75.

Expression and Purification of EF-Ts. A construct for EF-Ts expression as a fusion protein with the intein self-splicing element and chitin binding domain in the IMPACT I system (NE Biolabs) was kindly provided by Charlotte Knudsen (Aarhus). The protein was expressed in *E. coli* B834 DE3 cells for 1 h after induction with IPTG at 30 °C. Cells were opened by sonication in buffer B. After centrifugation at 15000*g*, the supernatant was mixed with a suspension of chitin beads equilibrated with buffer B. After incubation for 30 min on ice, chitin beads were washed three times with buffer B and five times with buffer F (20 mM Tris-HCl, pH 8.0, 0.1 mM EDTA, 50 mM NaCl). Cleavage of the intein tag was performed by incubation in buffer G (20 mM Tris-HCl, pH 8.0, 0.1 mM EDTA, 50 mM NaCl, 60 mM DTT, 0.4 KCl) for about 30 h at 20 °C, and EF-Ts was eluted from the beads with buffer G without DTT. EF-Ts was further purified by gel filtration on Superdex 75 in buffer A, shock-frozen in liquid nitrogen, and stored at −80 °C.

Concentration Measurements. EF-Tu concentrations were determined photometrically at 280 nm using a molar extinction coefficient of $\epsilon = 32900$ M^{-1} cm^{-1} (*21*). EF-Ts was measured by absorbance at 210 nm (*22*) or 205 nm (*23*). Concentrations were verified by comparing the intensity of the Coomassie-stained protein band on a 12% SDS−PAGE with that of a standard protein (EF-Tu or EF-Ts) using an imaging densitometer (GS-700).

Rapid Kinetic Measurements. Fluorescence stopped-flow measurements were performed on a SX-18MV spectrometer (Applied Photophysics) as described previously (*24*−*26*). Tryptophan fluorescence was excited at 280 nm and measured after passing KV335 filters (Schott). Fluorescence of mant-GDP was excited either directly at 349 nm or via

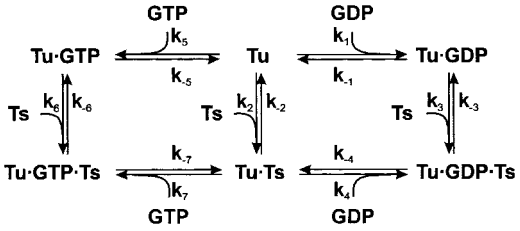

FIGURE 1: Kinetic mechanism of nucleotide exchange in EF-Tu.

fluorescence resonance energy transfer (FRET) from tryptophan excited at 280 nm and measured after passing KV408 filters (Schott). Experiments were performed in buffer A at 20 °C by rapidly mixing equal volumes (60 μL each) of reactants and monitoring the time course of the fluorescence change. Time courses depicted in the figures were obtained by averaging 5−10 individual transients. Data were evaluated by fitting to an exponential function with a characteristic apparent time constant (k_{app}), amplitude (A), and another variable for the final signal (F_∞) according to the equation $F = F_\infty + A \exp(-k_{app}t)$, where F is the fluorescence at time t. Calculations were performed using TableCurve software (Jandel Scientific). Standard deviations for apparent constants k_{app} were calculated using the same software. Numerical integration was carried out using Scientist for Windows software (MicroMath). All elemental rate constants of nucleotide exchange, except k_{-2}, were measured directly. The value of k_{-2} was calculated from all other rate constants according to the model depicted in Figure 1. Standard deviations of the rate constants were estimated from the variation of the values obtained from several experiments.

RESULTS

The schematic mechanism of EF-Ts-catalyzed nucleotide exchange in EF-Tu is given in Figure 1. EF-Tu can bind GDP (association rate constant k_1), GTP (k_5), or EF-Ts (k_2) to form the respective binary complexes which dissociate with the respective rate constants k_{-1}, k_{-5}, and k_{-2}. EF-Ts stimulates the low intrinsic dissociation rate of the EF-Tu·nucleotide complex by the formation of the ternary complex, EF-Tu·nucleotide·EF-Ts. The interaction of EF-Tu·GDP or EF-Tu·GTP with EF-Ts can be described by two consecutive equilibria that represent the formation of the ternary complex and the release of the nucleotide, respectively. EF-Ts reversibly interacts with EF-Tu·GDP to form the ternary complex EF-Tu·GDP·EF-Ts (k_3 and k_{-3}). GDP can be released from the ternary complex into solution (k_{-4}), from where it can rebind to the binary complex EF-Tu·EF-Ts (k_4). By analogy, EF-Tu·GTP can bind EF-Ts (k_6), and the ternary complex can dissociate into either EF-Tu·GTP and EF-Ts (k_{-6}) or EF-Tu·EF-Ts and GTP (k_{-7}). The binding of GTP to the binary complex EF-Tu·EF-Ts is characterized by k_7. Note that rate constants k_1−k_7 are bimolecular association constants (M^{-1} s^{-1}), whereas rate constants k_{-1}−k_{-7} are dissociation constants (s^{-1}). Table 1 summarizes the experiments that were carried out and the observables used, as well as the fitting parameters that lead to the kinetic constants.

Interaction of GDP/GTP with EF-Tu (k_1, k_{-1}, k_5, k_{-5}). GDP/GTP binding to EF-Tu was studied essentially as described (*14*) using FRET from Trp184 in EF-Tu to mant-GDP/mant-GTP, which results in an increase of mant fluorescence upon binding of the nucleotide to the factor. To measure the association rate constants, k_1 and k_5, nucleotide-free EF-Tu was used. Time courses of binding were measured at a constant concentration of EF-Tu and varying excess concentrations of mant-GDP/mant-GTP (Figure 2A). The data were analyzed by exponential fitting to determine the value of k_{app} for each titration point, and k_1 was determined from the slope of the linear dependence of k_{app} on the concentration of mant-GDP/mant-GTP (Figure 2B). The values obtained were $k_1 = (2 \pm 0.5) \times 10^6$ M^{-1} s^{-1} and $k_5 = (5 \pm 1) \times 10^5$ M^{-1} s^{-1}.

Nucleotide dissociation from EF-Tu·GDP (k_{-1}) and EF-Tu·GTP (k_{-5}) was studied in the presence of excess mant-GDP/mant-GTP using FRET (Figure 2C). In this case, the rate of mant-GDP/GTP binding is limited by the rate of dissociation of unlabeled nucleotide from EF-Tu; in the presence of a large excess of mant-labeled nucleotide, rebinding of unlabeled nucleotide is negligible, whereas the binding of mant-GDP/mant-GTP is very fast. Thus, the rate by which the fluorescence increases equals the dissociation rate constant of the unlabeled nucleotide. The values obtained by single-exponential fitting of the time courses shown in Figure 2C were $k_{-1} = 0.002 \pm 0.001$ s^{-1} and $k_{-5} = 0.03 \pm 0.01$ s^{-1} for EF-Tu·GDP and EF-Tu·GTP, respectively. The same value of k_{-1} was obtained for the dissociation of EF-Tu·mant-GDP in the presence of a large excess of unlabeled GDP upon direct excitation of mant fluorescence (data not shown). In this case, a fluorescence decrease was observed, because the fluorescence of mant-GDP in the EF-Tu·mant-GDP complex is about 30% higher than that of free mant-GDP (*8*, *27*). The values of the association and dissociation rate constants are consistent with those previously obtained for EF-Tu from *E. coli* using nitrocellulose filtration (*28*, *29*) or from *T. thermophilus* using the stopped-flow technique (*14*).

Dissociation of EF-Tu·GDP in the Absence of Bound Mg^{2+}. To study the contribution of Mg^{2+} coordination to nucleotide binding, we measured the dissociation of EF-Tu·GDP in the presence of 10 mM EDTA (Figure 3). The EF-Tu·mant-GDP complex was preincubated with 10 mM EDTA for 5 min at 37 °C and rapidly mixed with 10 mM EDTA in the presence of 25 μM GDP to avoid rebinding of mant-GDP. The rate constant of dissociation was 0.30 ± 0.1 s^{-1}. When EF-Tu·mant-GDP was rapidly mixed with 10 mM EDTA together with excess unlabeled nucleotide without prior incubation, the dissociation rate constant was 0.6 ± 0.1 s^{-1}. A similar result, 0.5 ± 0.1 s^{-1}, was obtained when the dissociation of unlabeled GDP from EF-Tu·GDP was measured by adding excess mant-GDP and EDTA and exciting mant fluorescence via FRET (data not shown). Thus, the removal of Mg^{2+} from EF-Tu·GDP accelerates the dissociation of GDP by a factor of 150−300.

Upon 2-fold dilution of the EF-Tu·mant-GDP complex formed in a 3-fold excess of mant-GDP in the presence of 10 mM EDTA (Figure 3), the rate of reaction, k_{app}, and the portion of the nucleotide remaining in the complex at equilibrium depends on both association and dissociation rate constants and concentrations of ligands. The value of k_1 was determined by numerical integration using both time courses shown in Figure 3. The association rate constant k_1 in the absence of Mg^{2+} was $(9 \pm 1) \times 10^5$ M^{-1} s^{-1}, about 2 times slower compared to the value obtained in the presence of Mg^{2+}, $(2 \pm 0.5) \times 10^6$ M^{-1} s^{-1}.

Table 1: Determination of the Rate Constants of Interactions between EF-Tu, EF-Ts, and Guanine Nucleotides

ligand		fluorescence	concn	data fitting	
constant	variable	signal	dependence	parameters	values
nucleotide-free EF-Tu	mant-GDP	mant (FRET)	linear	slope = k_1	$(2 \pm 0.5) \times 10^6$ M^{-1} s^{-1}
				Y-intercept = k_{-1}	close to 0
nucleotide-free EF-Tu	mant-GTP	mant (FRET)	linear	slope = k_5	$(5 \pm 1) \times 10^5$ M^{-1} s^{-1}
				Y-intercept = k_{-5}	close to 0
nucleotide-free EF-Tu	EF-Ts	Trp184	linear	slope = k_2	$(1 \pm 0.2) \times 10^7$ M^{-1} s^{-1}
				Y-intercept = k_{-2}	close to 0
EF-Tu·GDP	mant-GDP	mant (FRET)	none	$k_{app} = k_{-1}$	0.002 ± 0.001 s^{-1}
EF-Tu·GTP	mant-GTP	mant (FRET)	none	$k_{app} = k_{-5}$	0.03 ± 0.01 s^{-1}
EF-Tu·mant-GDP	EF-Ts, excess GDP	mant	hyperbolic	initial slope = $k_3/(1 + k_{-3}/k_{-4})$	1.6×10^7 M^{-1} s^{-1}
				k_{app} at saturation = k_{-4}	125 ± 25 s^{-1}
EF-Tu·EF-Ts	GDP	Trp184	hyperbolic	initial slope = $k_4/(1 + k_{-4}/k_{-3})$	1.0×10^7 M^{-1} s^{-1}
				k_{app} at saturation = k_{-3}	350 ± 50 s^{-1}
EF-Tu·mant-GTP	EF-Ts, excess GDP	mant	hyperbolic	initial slope = $k_6/(1 + k_{-6}/k_{-7})$	2.0×10^7 M^{-1} s^{-1}
				k_{app} at saturation = k_{-7}	85 ± 10 s^{-1}
EF-Tu·EF-Ts	GTP	Trp184	hyperbolic	initial slope = $k_7/(1 + k_{-7}/k_{-6})$	2.5×10^6 M^{-1} s^{-1}
				k_{app} at saturation = k_{-6}	60 ± 10 s^{-1}
EF-Tu·EF-Ts	mant-GTP	mant	linear part	slope = $k_7/(1 + k_{-7}/k_{-6})$	2.3×10^6 M^{-1} s^{-1}

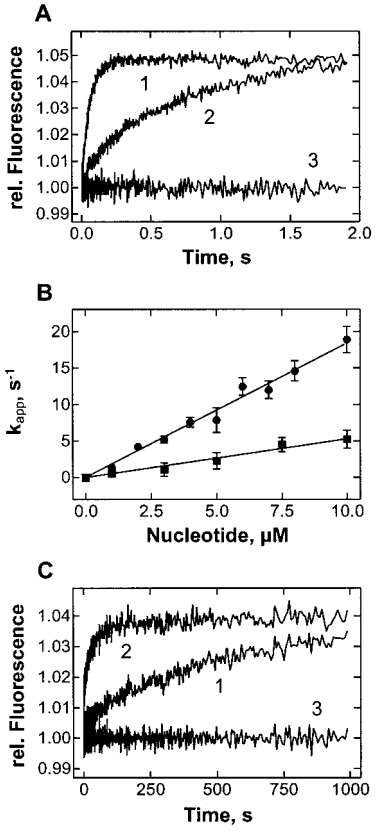

FIGURE 2: Interaction of guanine nucleotides with EF-Tu in the absence of EF-Ts. (A) Time courses of (1) mant-GDP (5 μM) or (2) mant-GTP (5 μM) binding to nucleotide-free EF-Tu (0.5 μM) measured by FRET excitation of mant fluorescence; (3) control without factor. (B) Concentration dependence of k_{app}. k_{app} values were calculated by single-exponential fitting from time courses as in (A). Key: circles, mant-GDP; squares, mant-GTP. (C) Dissociation of (1) GDP or (2) GTP from EF-Tu·GDP or EF-Tu·GTP (0.5 μM) in the presence of the respective mant nucleotide in excess (25 μM); (3) control with EF-Tu·GDP (0.5 μM) in the absence of mant-GDP. Mant fluorescence was excited by FRET.

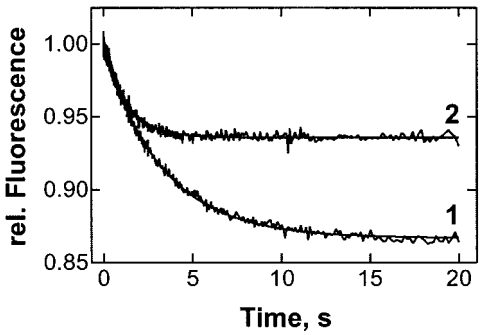

FIGURE 3: Effect of Mg^{2+}. Dissociation of the EF-Tu·mant-GDP complex (0.3 μM) in the presence of 10 mM EDTA and 25 mM GDP (1) or in the absence of GDP (2). Smooth lines are calculated from the values of k_1 and k_{-1} determined by numerical integration, 9×10^5 M^{-1} s^{-1} and 0.3 s^{-1}, respectively.

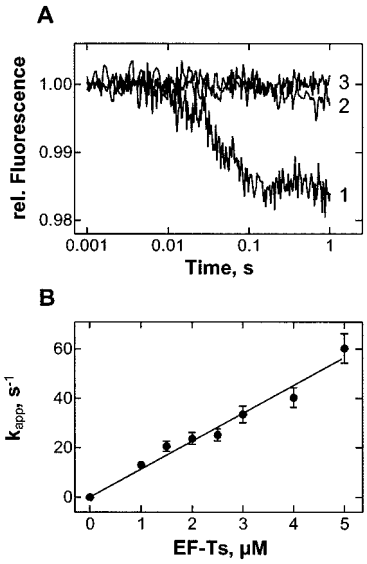

FIGURE 4: EF-Tu·EF-Ts interactions. (A) Fluorescence changes of Trp184 in EF-Tu (0.5 μM) upon addition of EF-Ts (1.5 μM) (1), GDP (25 μM) (2), or buffer (3). (B) Concentration dependence of the rate of EF-Tu·EF-Ts complex formation.

Binding of EF-Tu to EF-Ts (k_2). The formation of the EF-Tu·EF-Ts complex was monitored by the change of the intrinsic tryptophan fluorescence of EF-Tu. Upon binding of EF-Ts to nucleotide-free EF-Tu, a fluorescence decrease was observed (Figure 4A). Although the fluorescence change was small (about 2%), an average of 5−10 transients gave a signal-to-noise ratio which was sufficient for reliable single-exponential fitting. To determine the association constant, time courses were measured at increasing concentrations of EF-Ts, and the value of k_2 was determined from the slope

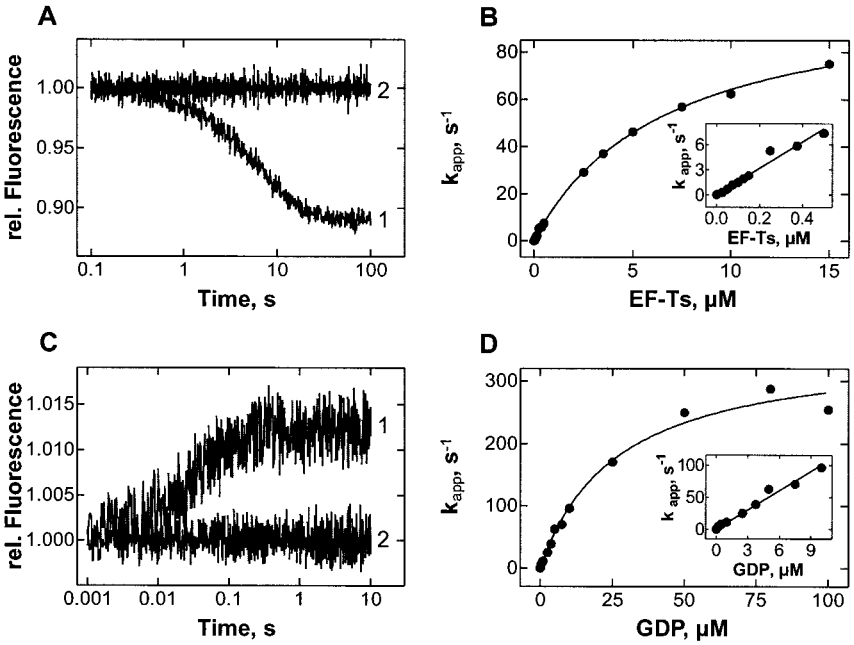

FIGURE 5: Interaction of EF-Tu with EF-Ts and GDP. (A) Time course of dissociation of EF-Tu·mant-GDP (0.15 μM) in the presence of EF-Ts (0.1 μM) and excess unlabeled GDP (25 μM) (1) or in the absence of EF-Ts (2). The fluorescence of the mant group was monitored. (B) Concentration dependence of k_{app}. The values of k_{app} were calculated by single-exponential fitting from the time courses as in (A). (C) Time course of dissociation of EF-Tu·EF-Ts (0.5 μM) in the presence of GDP (2.5 μM) (1) or in the absence of the nucleotide (2). The fluorescence of Trp184 in EF-Tu was monitored. (D) Concentration dependence of k_{app}. The values of k_{app} were calculated by single-exponential fitting from the time courses as in (B).

of the linear dependence of k_{app} on EF-Ts concentration (Figure 4B). The value of the association rate constant of EF-Tu with EF-Ts was $k_2 = (1 \pm 0.2) \times 10^7$ M^{-1} s^{-1}. The intercept with the *Y*-axis was close to zero, and thus k_{-2} could not be determined with precision.

Interaction of EF-Tu with EF-Ts in the Presence of GDP (k_3, k_{-3}, k_4, k_{-4}). To study the EF-Ts-catalyzed dissociation of GDP from EF-Tu·GDP, experiments were carried out with mant-GDP. The fluorescence of mant was excited directly. Upon mixing of EF-Tu·mant-GDP with EF-Ts, a single-exponential fluorescence decay was observed due to dissociation of the nucleotide (Figure 5A). Titrations were performed at a constant concentration of EF-Tu·mant-GDP and increasing concentrations of EF-Ts. An excess of unlabeled GDP was added together with EF-Ts to avoid rebinding of mant-GDP. At low concentrations of EF-Ts, k_{app} increased linearly, indicating that the formation of the EF-Tu·mant-GDP·EF-Ts complex was rate limiting (Figure 5B). At high concentrations of EF-Ts, the rate of the reaction reached saturation; because the rebinding of mant-GDP to EF-Tu·EF-Ts is excluded by the presence of excess unlabeled GDP, the rate at saturation equals k_{-4}. Fitting a hyperbolic curve to the data gives the value of $k_{-4} = 125 \pm 25$ s^{-1}. At low concentrations of EF-Ts, the initial slope of the titration curve (inset in Figure 5B) is equal to $k_3/(1 + k_{-3}/k_{-4})$ (*30*). Thus the value of k_3 can be calculated, provided both k_{-4} and k_{-3} are known.

To determine k_{-3}, titrations were carried out with a fixed concentration of the purified EF-Tu·EF-Ts complex and increasing concentrations of GDP. In this case, the change in intrinsic tryptophan fluorescence was monitored, which reflects the binding of EF-Tu to EF-Ts and is insensitive to the nucleotide binding (Figure 4A). The rates of EF-Ts dissociation were determined from the time courses (Figure 5C) by single-exponential fitting and plotted as a function of GDP concentration (Figure 5D). The value of k_{-3} estimated by fitting the data to a hyperbolic function was 350 ± 50 s^{-1}. The contribution of the reverse reaction, i.e., rebinding of EF-Ts to the EF-Tu·GDP complex, determined by k_3[EF-Ts], is negligible at saturating concentrations of GDP, because the concentration of free EF-Ts does not exceed the initial concentration of the EF-Tu·EF-Ts complex, 0.5 μM. The initial slope of the curve (inset in Figure 5D) is $k_4/(1 + k_{-4}/k_{-3})$. From the initial slopes of Figure 5B,D and the determined values of k_{-3} and k_{-4}, the remaining rate constants were calculated as $k_3 = (6 \pm 1) \times 10^7$ M^{-1} s^{-1} and $k_4 = (1.4 \pm 0.5) \times 10^7$ M^{-1} s^{-1} (Table 1).

These values of the kinetic constants are close to those reported previously by Hwang and Miller for the dissociation rate constant [k_{-4} can be extrapolated to 120 s^{-1} at 20 °C (*6*)] and by Eccleston et al. for the bimolecular rate constants [k_3 and k_4 about 10^7 (*8*)] but are about 10 times lower that those determined by rapid filtration (*4*). Most probably, the reason for the discrepancy is the use in the latter work of a nonequilibrium filtration technique in which the rapid application of a sample onto the filter was followed by a slow washing step. As part of the labile EF-Tu·GDP·EF-Ts complexes may dissociate during the washing step, the technique tends to yield artificially high exchange rates.

Interaction of EF-Tu with EF-Ts in the Presence of GTP (k_6, k_{-6}, k_7, k_{-7}). The interactions of EF-Tu, EF-Ts, and GTP were studied in the same way as described above for GDP, except that GTP solutions were preincubated with phosphoenolpyruvate and pyruvate kinase in order to convert any GDP present to GTP. Dissociation of GTP from EF-Tu in the presence of EF-Ts was monitored by the fluorescence of mant-GTP (Figure 6A; Table 1). Titrations were done at constant concentrations of EF-Tu·mant-GTP and increasing concentrations of EF-Ts in the presence of excess unlabeled nucleotide (Figure 6B), and $k_{-7} = (85 \pm 10)$ s^{-1} was

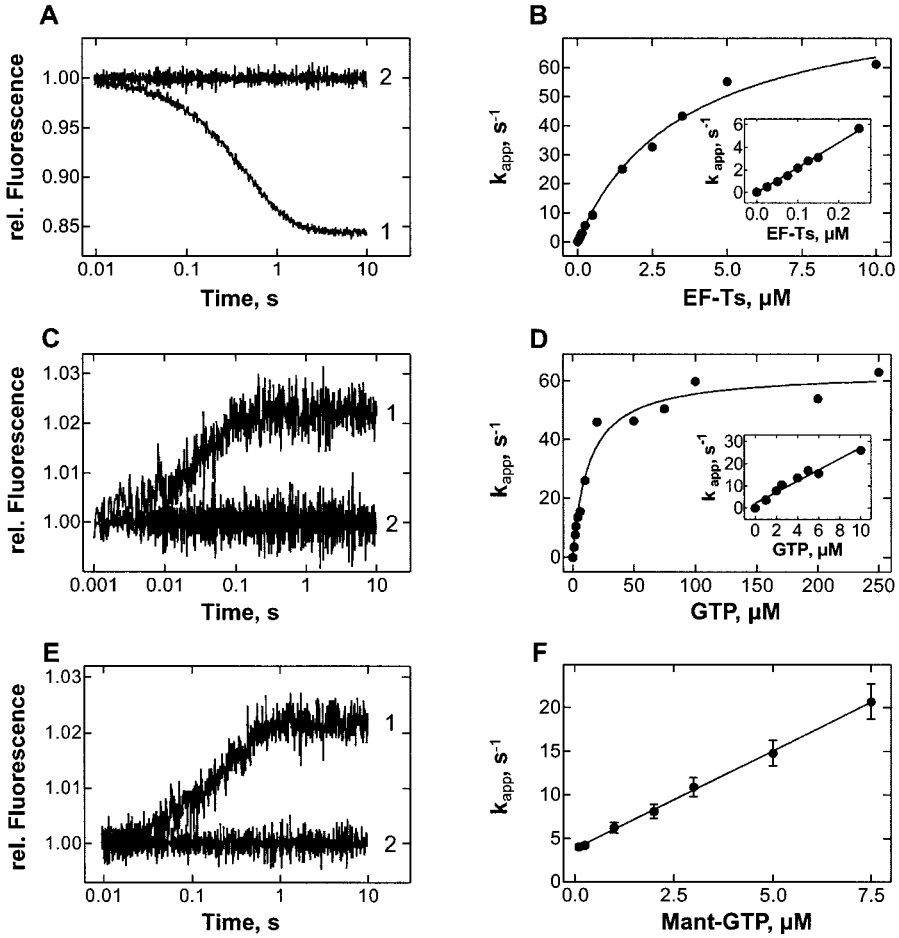

FIGURE 6: Interaction of EF-Tu with EF-Ts and GTP. (A) Time course of dissociation of EF-Tu·mant-GTP (0.15 μM) in the presence of EF-Ts (0.1 μM) and excess unlabeled GTP (25 μM) (1) or in the absence of EF-Ts (2). The fluorescence of mant was monitored. GTP and mant-GTP solutions were preincubated with phosphoenolpyruvate and pyruvate kinase to minimize the contamination with GDP. (B) Concentration dependence of k_{app}. The values of k_{app} were calculated by single-exponential fitting from the time courses as in (A). (C) Time course of dissociation of EF-Tu·EF-Ts (0.5 μM) in the presence of GTP (10 μM) (1) or in the absence of the nucleotide (2). The fluorescence of Trp184 in EF-Tu was monitored. The EF-Tu·EF-Ts complex was purified by gel filtration. Stock solutions of GTP (4−40 mM) were preincubated with phosphoenolpyruvate and pyruvate kinase and then diluted such that their final concentrations did not exceed 0.02 mM and 0.7 μg/mL, respectively. (D) Concentration dependence of k_{app}. The values of k_{app} were calculated by single-exponential fitting from the time courses as in (B). (E) Time course of binding of EF-Tu·EF-Ts (0.5 μM) to mant-GTP (0.25 μM) (1) and mant-GTP in the absence of factors (2). (F) The concentration dependence of k_{app} was determined in experiments analogous to those of panel E.

determined at saturation by fitting the data to a hyperbolic function. When the GTP-induced dissociation of EF-Tu·EF-Ts was monitored by tryptophan fluorescence (Figure 6C), $k_{-6} = 60 \pm 10$ s^{-1} was estimated at saturation with GTP (Figure 6D). Rate constants $k_6 = (3 \pm 0.5) \times 10^7$ M^{-1} s^{-1} and $k_7 = (6 \pm 1) \times 10^6$ M^{-1} s^{-1} were calculated from the initial slopes of Figure 6B,D and values of k_{-6} and k_{-7}, as described above for GDP.

As the changes of tryptophan fluorescence upon dissociation of EF-Tu·EF-Ts were small, the value of k_7 was confirmed by a different approach. EF-Tu·EF-Ts was rapidly mixed with mant-GTP in the presence of phosphoenolpyruvate and pyruvate kinase, and the increase of mant fluorescence brought about by mant-GTP binding was monitored by FRET (Figure 6E). The value of k_{app} increased linearly with mant-GTP concentration with a slope of 2.3×10^7 M^{-1} s^{-1} (Figure 6F), the same value as measured by tryptophan fluorescence, 2.5×10^7 M^{-1} s^{-1} (inset in Figure 6D); in both cases, the slope of the plot equals $k_7/(1 + k_{-7}/k_{-6})$ (Table 1).

Calculation of k_{-2}. The rate constant of EF-Tu·EF-Ts dissociation was the only constant which could not be measured directly and was therefore calculated on the basis of other rate constants and the law of mass action. From the rate constants of the right [$k_{-2} = k_{-1}k_2k_{-3}k_4/(k_1k_3k_{-4})$] and left [$k_{-2} = k_{-5}k_2k_{-6}k_7/(k_5k_6k_{-7})$] part of the scheme in Figure 1, values for k_{-2} were calculated as 0.007 s^{-1} and 0.08 s^{-1}, respectively. The equilibrium dissociation constants of EF-Tu·EF-Ts, K_2, calculated from these values and $k_2 = 1 \times 10^7$M^{-1} s^{-1}, were 0.7×10^{-9} and 7×10^{-9} M, comparable to previously reported values around 10^{-9} M (*31*−*33*). Given the standard deviations of the rate constants used for the calculation, the difference of the two values of k_{-2} is statistically insignificant. From the equilibrium constant of EF-Tu binding to EF-Ts reported for similar experimental conditions, 1.1×10^{-9} M (*32*), and the present value of $k_2 = 1 \times 10^7$ M^{-1} s^{-1}, a value of $k_{-2} = 0.01$ s^{-1} is calculated. Thus, a realistic value for the rate constant of EF-Tu·EF-Ts dissociation is $k_{-2} = 0.03$ s^{-1}, obtained by averaging the three estimates for k_{-2}, 0.007 s^{-1}, 0.08 s^{-1}, and 0.01 s^{-1}.

DISCUSSION

Effect of EF-Ts on the Interaction of EF-Tu with Guanine Nucleotides. Figure 7 summarizes the kinetic parameters

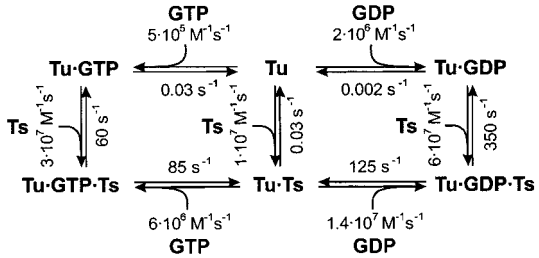

FIGURE 7: Summary of the rate constants of EF-Tu interactions with EF-Ts and guanine nucleotides.

obtained for the interactions between EF-Tu, EF-Ts, and guanine nucleotides. In the absence of EF-Ts, both binding of GDP or GTP to and dissociation from EF-Tu are very slow. The association rate constants, k_1 and k_5, are about 10^6 M^{-1} s^{-1}, which is 2 orders of magnitude lower than expected for a diffusion-controlled reaction. This indicates that the diffusion-controlled formation of the complex is followed by a conformational change in EF-Tu, which stabilizes nucleotide binding and is probably the reason for the change of mant fluorescence. In the absence of EF-Ts, the rearrangement is slow; the low dissociation rate constants suggest that the structure of the resulting complex is such as to occlude the nucleotide in a kinetically stable EF-Tu·GDP/GTP complexes. Binding of EF-Ts to EF-Tu leads to a 10-fold increase of the rates of nucleotide binding, k_4 and k_7. Furthermore, the rate constants of GDP/GTP dissociation from the respective ternary complexes, k_{-4} and k_{-7}, are increased by factors of 6×10^4 (GDP) and 3×10^3 (GTP). This suggests that, in the ternary complexes, the nucleotide binding pocket of EF-Tu is open and allows rapid association and dissociation of the nucleotide. On the other hand, EF-Ts is bound less tightly in the ternary complexes than in the binary complex EF-Tu·EF-Ts, indicating that the complexes are structurally different. Thus four different structures of EF-Tu can be distinguished: conformations which form tight complexes with nucleotides (GDP- and GTP-bound forms) (*34*−*37*) or EF-Ts (EF-Ts-bound form) (*1*, *2*) and a fourth conformation which is characterized by labile binding of both nucleotide and EF-Ts and which has not been characterized structurally so far.

Another interesting implication of the data is that the bimolecular rate constant of EF-Ts binding to EF-Tu is more or less independent of the nucleotide binding state of EF-Tu (Figure 7). This suggests that structural determinants for the association are located outside the nucleotide binding pocket of EF-Tu, which has markedly different structures in the GDP- and GTP-bound forms. Besides the nucleotide binding site, there are two regions of contact in the EF-Tu·EF-Ts complex, i.e., helix D in domain 1 of EF-Tu, which interacts with the N-terminal domain of EF-Ts, and the tip of domain 3 of EF-Tu, which is bound to subdomain C of the core of EF-Ts (*1*). The orientation of domain 3 is different in EF-Tu·GDP and EF-Tu·GTP, and thus the interaction of EF-Ts with this part of EF-Tu should be influenced by the nucleotide. Thus, the most likely candidate for the initial contact is helix D of EF-Tu, and the interactions of EF-Ts with EF-Tu in the vicinity of the nucleotide binding site and in domain 3 are likely to be established at later stages of complex formation. In *E. coli* EF-Tu·EF-Ts, these rearrangements are rapid and are not observed as separate kinetic steps.

Effect of Mg^{2+}. Disruption of the Mg^{2+} binding site in EF-Tu by EF-Ts was proposed to be an important factor in facilitating the nucleotide release (*1*, *2*). The rate constant of GDP release from EF-Tu·GDP was increased 150−300-fold upon removal of Mg^{2+} by EDTA, compared to a 6×10^4-fold enhancement by EF-Ts. This suggests that the loss of Mg^{2+} coordination is not the only factor responsible for the acceleration of nucleotide dissociation from EF-Tu·EF-Ts. Other factors, such as the EF-Ts-induced structural rearrangement in the P loop (*1*−*3*) and possibly changes in the interactions of EF-Tu with the guanine base and ribose moieties of the nucleotides (*1*) also contribute significantly to the destabilization of nucleotide binding to EF-Tu.

Kinetic Mechanism of Nucleotide Exchange. The concentration of GTP in the cell is about 10 times that of GDP, 0.9 mM and 0.1 mM, respectively (*38*). From the kinetic data, equilibrium dissociation constants of 10^{-9} M and 6×10^{-8} M are obtained for EF-Tu·GDP and EF-Tu·GTP in the absence of EF-Ts, respectively (Figure 7). Thus, GTP can displace EF-Tu-bound GDP under equilibrium conditions when GTP is in large excess. In the complete translation system, EF-Tu·GTP forms a strong complex (nanomolar) with aminoacyl-tRNA, which strongly shifts the equilibrium toward the GTP-bound species but does not affect the kinetics of the nucleotide exchange. The rate of spontaneous GDP dissociation, 0.002 s^{-1}, is much too slow to sustain a rate of protein elongation of about 10 s^{-1}, even though EF-Tu is present in 10-fold excess over ribosomes. In the presence of EF-Ts, dissociation of GDP is much faster, although the equilibrium between EF-Tu·GDP and EF-Tu·GTP is unchanged. The concentration of EF-Tu is about 100 μM in exponentially growing cells, whereas the concentration of EF-Ts approximately equals that of the ribosomes, about 10 μM (*38*); assuming all ribosomes to be active in translation, the concentration of EF-Tu·GDP immediately after release from the ribosome is expected to be the same or lower. Under these conditions, the rate of EF-Ts binding to EF-Tu·GDP, as calculated from the values of k_3, k_{-3}, and k_{-4}, is about 158 s^{-1} [rate $= k_3$[EF-Ts]$/(1 + k_{-3}/k_4)$], and the dissociation of GDP from the ternary complex proceeds at 100 s^{-1} [rate $= k_{-4}/[1 + (k_4$[GDP]$)/(k_7$[GTP]$)]$]. Together, these two reactions take about 16 ms (1/158 + 1/100 s), which corresponds to a rate of about 60 s^{-1} for the formation of the binary complex EF-Tu·EF-Ts. The following step of GTP binding is extremely fast (>2000 s^{-1}), due to the high cellular concentration of GTP, whereas the dissociation of EF-Ts may be expected at 57 s^{-1} [rate $= k_{-6}/[1 + (k_6$[EF-Ts]$)/k_{\text{aa-tRNA binding}}$[aa-tRNA]$]]$, assuming that EF-Tu·GTP binds aminoacyl-tRNA with an association rate constant of 5×10^7 M^{-1} s^{-1} (W. Wintermeyer, unpublished data) and that the concentrations of free EF-Tu and aminoacyl-tRNA in the cell are about equal. Together, all steps of the nucleotide exchange in EF-Tu take about 30 ms, 16 ms for the release of GDP and 18 ms for GTP binding and dissociation of EF-Ts, and the overall rate of the complete cycle of nucleotide exchange is expected to be about 30 s^{-1}. This value is fully compatible with the rate of protein synthesis in vivo, about 10 s^{-1}, and in excellent agreement with the previously reported number for the turnover of EF-Tu (*10*, *11*). Thus, there is no single rate-limiting step in the mechanism of nucleotide exchange in EF-Tu; rather, three steps, i.e., EF-Ts binding to EF-Tu·GDP, dissociation of GDP from EF-

Tu·GDP·EF-Ts, and dissociation of EF-Ts from EF-Tu·GTP·Ts, contribute about equally to the overall velocity of the reaction.

ACKNOWLEDGMENT

We thank Wolfgang Wintermeyer for critically reading the manuscript and for valuable suggestions, Charlotte Knudsen for the plasmid constructs coding for EF-Ts, and Petra Striebeck, Astrid Böhm, Carmen Schillings, Simone Möbitz, and Kornelia Kirse for expert technical assistance.

REFERENCES

1. Kawashima, T., Berthet-Colominas, C., Wulff, M., Cusack, S., and Leberman, R. (1996) *Nature 379*, 511−518.
2. Wang, Y., Jiang, Y. X., Meyering-Voss, M., Sprinzl, M., and Sigler, P. B. (1997) *Nat. Struct. Biol. 4*, 650−656.
3. Renault, L., Kuhlmann, J., Henkel, A., and Wittinghofer, A. (2001) *Cell 105*, 245−255.
4. Chau, V., Romero, G., and Biltonen, R. L. (1981) *J. Biol. Chem. 256*, 5591−5596.
5. Romero, G., Chau, V., and Biltonen, R. L. (1985) *J. Biol. Chem. 260*, 6167−6174.
6. Hwang, Y. W., and Miller, D. L. (1985) *J. Biol. Chem. 260*, 11496−11502.
7. Eccleston, J. F. (1984) *J. Biol. Chem. 259*, 12997−13003.
8. Eccleston, J. F., Kanagasabai, T. F., and Geeves, M. A. (1988) *J. Biol. Chem. 263*, 4668−4672.
9. Eccleston, J. F. (1981) *Biochemistry 20*, 6265−6272.
10. Ruusala, T., Ehrenberg, M., and Kurland, C. G. (1982) *EMBO J. 1*, 741−745.
11. Tapio, S., Bilgin, N., and Ehrenberg, M. (1990) *Eur. J. Biochem. 188*, 347−354.
12. Berger, W., Prinz, H., Striessnig, J., Kang, H. C., Haugland, R., and Glossmann, H. (1994) *Biochemistry 33*, 11875−11883.
13. Lenzen, C., Cool, R. H., Prinz, H., Kuhlmann, J., and Wittinghofer, A. (1998) *Biochemistry 37*, 7420−7430.
14. Wagner, A., Simon, I., Sprinzl, M., and Goody, R. S. (1995) *Biochemistry 34*, 12535−12542.
15. Lenzen, C., Cool, R. H., and Wittinghofer, A. (1995) *Methods Enzymol. 255*, 95−109.
16. Jameson, D. M., Gratton, E., and Eccleston, J. F. (1987) *Biochemistry 26*, 3894−3901.
17. Rodnina, M. V., Fricke, R., and Wintermeyer, W. (1994) *Biochemistry 33*, 12267−12275.
18. Arai, K. I., Kawakita, M., and Kaziro, Y. (1972) *J. Biol. Chem. 247*, 7029−7037.
19. John, J., Sohmen, R., Feuerstein, J., Linke, R., Wittinghofer, A., and Goody, R. S. (1990) *Biochemistry 29*, 6058−6065.
20. Klebe, C., Prinz, H., Wittinghofer, A., and Goody, R. S. (1995) *Biochemistry 34*, 12543−12552.
21. Block, W., and Pingoud, A. (1981) *Anal. Biochem. 114*, 112−117.
22. Tombs, M. P., Souter, F., and Maclagan, N. F. (1959) *Biochem. J. 73*, 167−171.
23. Scopes, R. K. (1974) *Anal. Biochem. 59*, 277−282.
24. Pape, T., Wintermeyer, W., and Rodnina, M. V. (2000) *Nat. Struct. Biol. 7*, 104−107.
25. Jagath, J. R., Rodnina, M. V., and Wintermeyer, W. (2000) *J. Mol. Biol. 295*, 745−753.
26. Knudsen, C., Wieden, H. J., and Rodnina, M. V. (2001) *J. Biol. Chem. 13*, 13.
27. Rodnina, M. V., Fricke, R., Kuhn, L., and Wintermeyer, W. (1995) *EMBO J. 14*, 2613−2619.
28. Fasano, O., Crechet, J. B., and Parmeggiani, A. (1982) *Anal. Biochem. 124*, 53−58.
29. Arai, K., Kawakita, M., and Kaziro, Y. (1974) *J. Biochem 76*, 293−306.
30. Fersht, A. (1998) *Structure and mechanism in protein science*, W. H. Freeman and Co., New York.
31. Zhang, Y., Sun, V., and Spremulli, L. L. (1997) *J. Biol. Chem. 272*, 21956−21963.
32. Zhang, Y., Yu, N.-J., and Spremulli, L. L. (1998) *J. Biol. Chem. 273*, 4556−4562.
33. Miller, D. L., and Weissbach, H. (1970) *Biochem. Biophys. Res. Commun. 38*, 1016−1022.
34. Abel, K., Yoder, M. D., Hilgenfeld, R., and Jurnak, F. (1996) *Structure 4*, 1153−1159.
35. Polekhina, G., Thirup, S., Kjeldgaard, M., Nissen, P., Lippmann, C., and Nyborg, J. (1996) *Structure 4*, 1141−1151.
36. Berchtold, H., Reshetnikova, L., Reiser, C. O., Schirmer, N. K., Sprinzl, M., and Hilgenfeld, R. (1993) *Nature 365*, 126−132.
37. Kjaersgard, I. V., Knudsen, C. R., and Wiborg, O. (1995) *Eur. J. Biochem. 228*, 184−190.
38. Neuhard, J., and Nygaard, P. (1987) *Purines and pyrimidines*, Vol. 1, American Society for Microbiology, Washington, DC.

BI015712W